

Relaxation Times of ^{31}P -Metabolites in Human Calf Muscle at 3 T

Martin Meyerspeer,¹ Martin Krššák,² and Ewald Moser^{1,3*}

Localized ^{31}P -STEAM experiments were performed at 3 T to estimate relaxation times of phosphorus-containing metabolites in the human calf muscle in vivo. T_1 and T_2 times of PCr, P_i , and NTPs were measured in the resting calf muscle of healthy subjects by varying TR and TE. The localization performance of the ^{31}P -STEAM sequence was evaluated on a test object, resulting in a relative selection efficiency of $78 \pm 1\%$ and contamination from outside the voxel of $0 \pm 2\%$ under fully relaxed conditions. T_1 relaxation times ($\pm\text{SD}$, $n = 5$) of P_i , PCr, γ -NTP, α -NTP, and β -NTP obtained at 3 T are 5.2 ± 1.0 s, 6.4 ± 0.2 s, 4.5 ± 0.3 s, 2.6 ± 0.9 s, and 3.5 ± 1.1 s, respectively. T_2 relaxation times ($\pm\text{SD}$, $n = 6$) of these metabolites are 148 ± 17 ms, 334 ± 30 ms, 78 ± 13 ms, 55 ± 7 ms, and 55 ± 10 ms, respectively. Spin-lattice relaxation times established at 3 T are consistent with literature data at lower field strengths, whereas spin-spin relaxation times are lower. Several methodological considerations are discussed which may help improve quantification of metabolite concentrations in the human (calf) muscle in vivo by using localized noninvasive ^{31}P -MRS at 3 T, which is currently being tested for routine clinical applications. Magn Reson Med 49:620–625, 2003. © 2003 Wiley-Liss, Inc.

Key words: 3 Tesla; STEAM; phosphorus; relaxation; human muscle

NMR spectra may be used to derive peak intensity ratios of tissue metabolites or even their absolute concentrations. To optimize signal-to-noise ratio (SNR) per unit time, in vivo spectra are often acquired with repetition times on the order of T_1 . In such a case, severe saturation effects have to be taken into account to allow quantification. T_1 values must, therefore, be known accurately. When the MRS signal is acquired as an echo, e.g., in localized spectroscopy, it should also be corrected for T_2 decay and phase modulation, in particular if coupled spin systems are observed. In addition, relaxation times are different for the various metabolites observed and may vary with the static magnetic field strength (B_0).

Phosphorus-NMR spectroscopy has become a useful tool for noninvasive investigation of muscle metabolism in vivo under various physiological and pathological conditions (1,2). Most ^{31}P metabolite relaxation times in human skeletal muscle published so far have been acquired at field strengths typical for clinical MR systems, i.e., 1.5 T (3–11), and a few at 2.0 T (12), or 2.35 T (13), while data at higher fields have been mostly obtained from animal studies. In view of the trend towards high-field whole-body NMR scanners also for routine clinical applications, it appears useful to measure metabolite relaxation times at higher field strength.

In the present study, apparent T_1 and T_2 of ^{31}P -containing metabolites in the human calf muscle were measured at 3 T, compared to literature data, and various factors affecting the accuracy and comparability are discussed.

METHODS

All experiments were performed on a 3 T Medspec S300 DBX whole-body scanner (Bruker Medical, Ettlingen, Germany), equipped with a passively shielded magnet (MagneX Scientific, Oxford, UK) and a BG-A55 wide-bore gradient coil system. For RF excitation and detection, a double-tuned surface coil (^1H : 125.6 MHz / ^{31}P : 50.85 MHz) with a diameter of 10 cm was used.

A ^{31}P -STEAM sequence (14,15) with sinc-shaped RF pulses truncated to three lobes was used to achieve exact spatial localization and outer volume suppression. The region selected was the resting soleus/gastrocnemius complex of young healthy subjects (total $n = 9$, age: 26.3 ± 6.4 years, four females, five males). Written informed consent was obtained from all volunteers before conducting the experiments, according to the guidelines of the local ethics committee. The nominal size of the cuboid-shaped VOI was set to $(5 \times 3.5 \times 7) \text{ cm}^3 = 122.5 \text{ cm}^3$, oriented along the muscle fibers, as shown in Fig. 1.

For positioning the VOI and estimation of the relative contribution of various muscle types, ^1H -gradient echo images were acquired in stacks of 20 axial slices using the same surface coil. The acquisition parameters were: matrix size = 256×192 , field of view (FOV) = $25.6 \text{ cm} \times 25.6 \text{ cm}$, slice thickness = 4 mm at TR = 480 ms, and TE = 7.4 ms.

The B_1 field distribution of the surface coil was estimated in a separate imaging experiment using a long pre-saturation pulse to rotate the magnetization vector several times in the region of interest. The test object was a cast in the shape of a human calf muscle, filled with vegetable oil to obtain a homogeneous volume while avoiding standing

¹NMR Group, Department of Medical Physics, Vienna University, Vienna, Austria.

²Department of Internal Medicine III, Division of Endocrinology and Metabolism, General Hospital of Vienna, Vienna, Austria.

³Department of Radiodiagnostics, General Hospital of Vienna, Vienna, Austria.

Grant sponsor: Austrian Science Fund; Grant number: FWF P15202; Grant sponsor: Österreichische Nationalbank.

*Correspondence to: Ewald Moser, Ph.D., Department of Medical Physics, Währingerstrasse 13, A-1090 Vienna, Austria.
E-mail: Ewald.Moser@univie.ac.at

Received 21 March 2002; revised 7 November 2002; accepted 14 November 2002.

DOI 10.1002/mrm.10426

Published online in Wiley InterScience (www.interscience.wiley.com).

© 2003 Wiley-Liss, Inc.

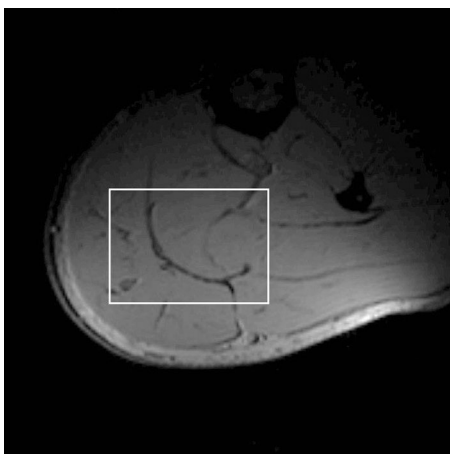


FIG. 1. Example of the VOI (5 cm (w) \times 3.5 cm (h) \times 7 cm (l)) positioned in the human soleus/gastrocnemius complex, selected with ^{31}P -STEAM.

RF wave effects. The RF pulse angle deviated less than $\pm 20\%$ from the ideal 90° pulse in 68% of the VOI and by at most -40% at the point of the VOI furthest from the RF coil. To demonstrate the effect of B_1 inhomogeneities on T_1 measurements, a large (5 \times 3.5 \times 7 cm^3) and a small (2 \times 1 \times 2 cm^3) VOI were positioned concentrically in a test object filled with 2 L of phosphate solution (100 mmol/l). Relaxation times measured in both VOIs were equal within error margins, i.e., $T_1 = 8.3 \pm 1.0$ s vs. $T_1 = 7.8 \pm 1.8$ s.

Localization Performance

The localization performance of the ^{31}P -STEAM sequence was estimated on a test object consisting of two compartments filled with test solutions (16). A cuboid box made of acrylic glass with a volume of 5 \times 3.5 \times 7 cm and a wall thickness of 1.2 mm was placed inside a vessel ($V = 1$ L) positioned on top of the $^1\text{H}/^{31}\text{P}$ -coil to simulate a VOI of equal size to the in vivo experiments. The cuboid compartment was filled with K_2HPO_4 solution doped with 1 $\mu\text{mol/l}$ MnCl_2 ($T_1 = 6.5 \pm 0.2$ s, measured in a separate inversion recovery experiment) and the outer vessel was filled with KH_2PO_4 solution without any relaxation agent ($T_1 = 6.0 \pm 0.2$ s), both at a concentration of 100 mmol/l. The contributions of signal originating from each compartment could be distinguished by their chemical shifts, which differed by ~ 3 ppm. A STEAM voxel was placed concentrically to the box and the localization performance of the sequence was examined by successively increasing the nominal VOI in 14 steps from 24.5 cm^3 to 245 cm^3 . Relative selection efficiency (E_{sel}) was defined as:

$$E_{\text{sel}} = 2 \frac{X}{A} \cdot 100\% \quad [1]$$

where X is the signal originating from inside the cube acquired with STEAM localization and A is the signal of the same compartment without localization, acquired in a one-pulse experiment. The factor of 2 was introduced in Eq. 1 as only 50% of the available z -magnetization can be

detected with STEAM, theoretically. Contamination (C) by signals arising from outside the VOI was defined as:

$$C = \frac{Y}{X + Y} \cdot 100\% \quad [2]$$

with Y designating the signal from the outer compartment acquired with STEAM. One series of spectra was acquired under fully relaxed conditions ($\text{TR} = 60$ s) with four averages, a second series was performed with $\text{TR} = 1$ s and 256 averages to simulate conditions of maximum saturation in our in vivo T_1 measurements. Echo time ($\text{TE} = 7.4$ ms) was the same as during the in vivo experiments.

In Vivo Measurements

Shimming the VOI positioned in the human calf muscle in vivo with Bruker's implementation of the FASTMAP (17) routine, using the proton signal, resulted in a line width (FWHM \pm SD) of the PCr signal in the ^{31}P -STEAM spectra of 6.5 ± 1.2 Hz, which allows discrimination of the NTP multiplets with $J \approx 18$ Hz. Exponential line broadening of 8 Hz and zero-filling to 8 k points was applied to the spectra for display only.

Relative contributions of the various muscle compartments were $58 \pm 9\%$, $30 \pm 10\%$, $11 \pm 6\%$, and $1.3 \pm 0.9\%$ for m. soleus, m. gastrocnemius, m. flexor hallucis longus, and m. plantaris, respectively.

T_1 was measured via progressive saturation (PS) experiments by varying TR in the STEAM experiment (ranging from 1 s to 18 s in 7 steps, $n = 5$), with the minimum TE of 7.4 ms. T_2 was measured by varying TE (ranging from 7.4 ms to 750 ms in 5–8 steps, $n = 6$), with TR = 5 s. In all measurements a middle period (TM) of 30 ms and a spectral width (SW) of 2500 Hz was chosen, with 1024 complex data points being acquired. To ensure steady-state conditions dummy scans were applied for 25 s, i.e., ~ 4 times the maximum T_1 expected, prior to data acquisition. The number of excitations (NEX) for each spectrum was adjusted to maintain similar SNRs for all spectra while varying TR or TE, i.e., NEX was as high as 512 for TR = 1 s and decreased to 32 for TR = 18 s in the T_1 measurements. For T_2 estimation of NTP, NEX was 256, at TE = 110 ms and TR = 5 s, to obtain $\text{SNR} \geq 3$ for these less abundant metabolites.

Spectral and Relaxation Time Data Processing

Quantification of the peak intensities was performed using the AMARES (18) time domain fit routine, as incorporated in the MRUI software package (19) (<http://carbon.uab.es/mrui/>). Gaussian lines were fitted to the resonances of inorganic phosphate (P_i), phosphocreatine (PCr), and nucleotide triphosphate (NTP, fitted as multiplets). Soft constraints were imposed on the phases after manual zero and first-order phasing (PCr: $\leq \pm 5^\circ$, P_i : $\leq \pm 20^\circ$, NTP: $\leq \pm 2^\circ$). Line widths (i.e., damping factors) and J -coupling constants of all NTP peaks were linked to each other and the intensities were set to be equal in the doublets and constrained to the ratio 1:2:1 for the β -NTP triplet.

Single exponential functions with three parameters for T_1 (20) and two parameters for T_2 of PCr and P_i were fitted

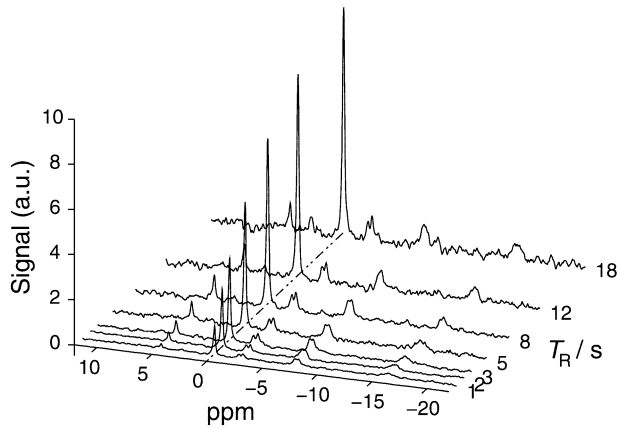


FIG. 2. Time series of a progressive saturation experiment for T_1 estimation of ^{31}P metabolites in human calf muscle in vivo at 3 T. The number of averaged acquisitions was increased for shorter TR to maintain similar SNRs in all scans. Exponential line broadening of 8 Hz and zero-filling to 8 k points was applied to the spectra for display only.

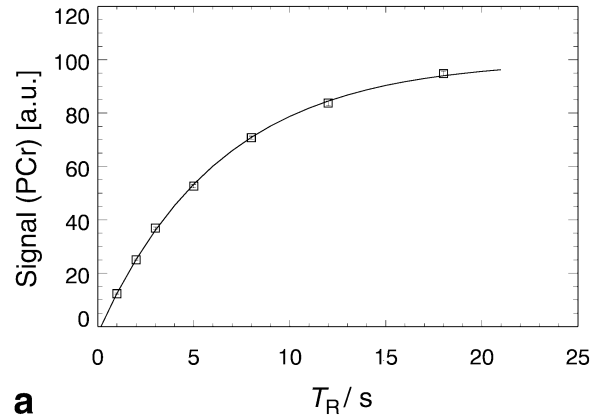
to the measured peak intensities using IDL (Research Systems, Boulder, CO, USA). Gaussian weighting was applied to the data points (i.e., $w = (1/\sigma_n)^2$), with σ_n representing the effective noise in the respective spectra, calculated from the intensities and standard deviations yielded by AMARES. If the STEAM sequence is used for acquisition, however, the NTP signal is subjected to phase modulation with varying TE, according to:

$$S(T_E) \text{ prop. } \cos^2\left(\frac{\pi J T_E}{2}\right) \quad [3]$$

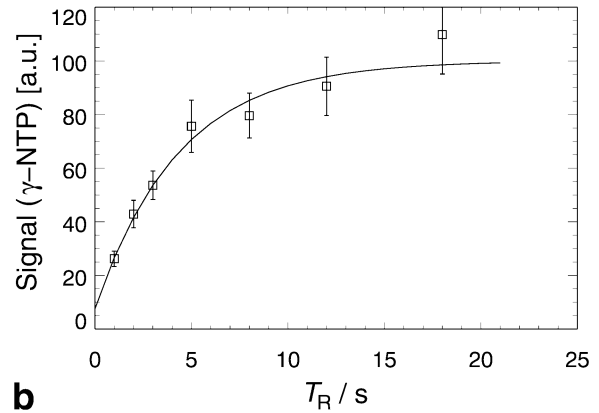
where $J = 18.2$ Hz. Therefore, T_2 of NTP was estimated from two echo times: 1) $TE_1 = 7.4$ ms (the minimum TE feasible); and 2) $TE_2 = 110$ ms, where the signal $S(TE)$ exhibits a local maximum (21). T_2 relaxation times were then calculated directly, using the equation:

$$T_2 = \frac{T_{E2} - T_{E1}}{\ln(S_1/S_2)} \quad [4]$$

after correcting for the signal loss of 4.3% at $T_{E1} = 7.4$ ms, according to Eq. [3].



a



b

FIG. 3. T_1 fit curves for (a) PCr ($r^2 = 0.9996$) and (b) γ -NTP ($r^2 = 0.9634$) in human calf muscle of a single subject ($V = 122.5$ ml, $TE = 7.4$ ms). Note that for PCr, error bars (± 1 SD) are smaller than the plot symbols.

RESULTS

Estimation of the localization performance with the two-compartment test object yielded a relative selection efficiency of $E_{\text{sel}} = 78 \pm 1\%$ and a contamination for the nominal size of the VOI adjusted to the volume of the acrylic glass cube of $C = 0 \pm 2\%$ under fully relaxed conditions. When performing these experiments with maximum saturation, i.e., using the shortest TR of the in vivo experiments, selection efficiency is decreased to $E_{\text{sel}} = 68 \pm 1\%$ and contamination increases to $C = 3 \pm 2\%$. These results demonstrate that the VOI is well defined, the fraction of undesired signal being zero inside the

Table 1
 T_1 Relaxation Times (s) in Human Calf Muscle In Vivo at 3 T

Subject	Gender	P_i	PCr	γ -NTP	α -NTP	β -NTP
1	F	6.4 ± 2.3	6.4 ± 0.2	4.1 ± 1.3	1.7 ± 0.5	2.1 ± 0.8
2	F	5.8 ± 1.1	6.3 ± 0.2	4.4 ± 1.4	1.6 ± 0.5	2.5 ± 1.2
3	M	3.8 ± 0.7	6.5 ± 0.2	4.7 ± 1.3	2.9 ± 0.8	4.7 ± 1.9
4	M	4.6 ± 1.1	6.1 ± 0.2	4.4 ± 1.5	3.8 ± 1.4	3.7 ± 2.4
5	M	5.2 ± 1.0	6.7 ± 0.2	4.9 ± 1.8	3.0 ± 1.0	4.4 ± 3.0
Mean \pm SD		5.2 ± 1.0	6.4 ± 0.2	4.5 ± 0.3	2.6 ± 0.9	3.5 ± 1.1

Errors given for each subject are individual standard deviations returned by the relaxation time fit routine. Also shown are the standard deviations of T_1 over all subjects.

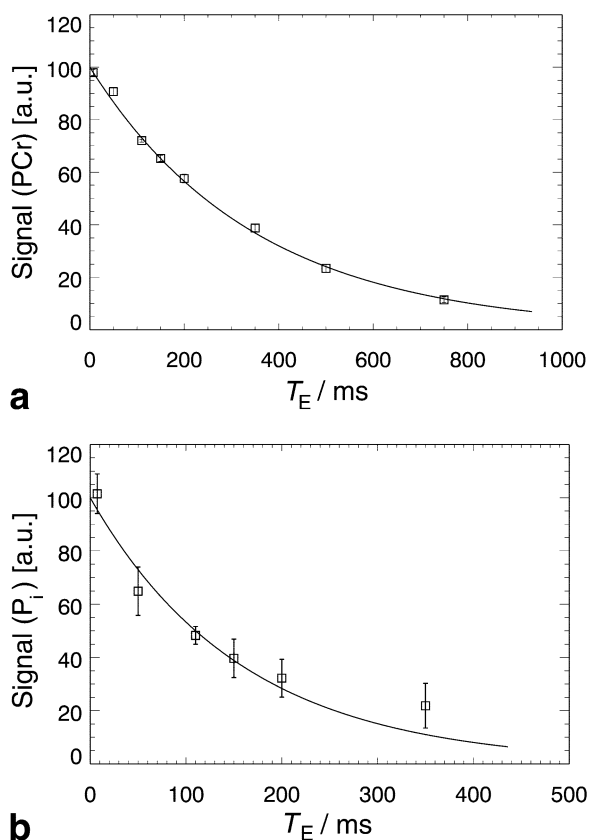


FIG. 4. T_2 fit curves for (a) PCr ($r^2 = 0.990$) and (b) P_i ($r^2 = 0.969$) in human calf muscle of a single subject ($V = 122.5$ ml, $\text{TR} = 5$ s). Note that for PCr, error bars (± 1 SD) are smaller than the plot symbols.

cube, and very low even within the cube walls (i.e., below the error margin of $\sim 2\%$ under relaxed conditions and only 3% at $\text{TR} = 1$ s).

A typical time series of localized ^{31}P -muscle spectra for T_1 estimation is shown in Fig. 2. Note that the noise level is lower for shorter TR, as the NEX is higher to obtain comparable SNR. No correction of baseline roll or removal of broad spectral components was required.

Typical T_1 fit curves for PCr and NTP of a single subject are shown in Fig. 3. Average Pearson's correlation coefficients for all fits are $r^2 = 0.9989 \pm 0.0008$ for PCr and range between $0.87 \leq r^2 \leq 0.96$ for the other metabolites.

Detailed results of all T_1 measurements of ^{31}P containing metabolites in resting human calf muscle at 3 T are summarized in Table 1.

T_2 fit curves of PCr and P_i are shown in Fig. 4. The fit quality is similar to T_1 , with $r^2 = 0.990 \pm 0.010$ for PCr and $r^2 = 0.969 \pm 0.034$ for P_i . NTP T_2 s were calculated from Eq. [4], without using any fit routine.

All T_2 relaxation times are summarized in Table 2.

DISCUSSION AND CONCLUSION

We present what are, to our knowledge, the first localized measurements of ^{31}P relaxation times of human muscle metabolites in vivo at 3 T. When comparing our results with published data acquired at lower field strengths, one also has to keep in mind the large number of RF-sequences used (i.e., various localization schemes and preparation of magnetization, e.g., PS, inversion, or saturation recovery), and the different types of RF coils and methods of fitting models to the data (e.g., exponential functions with two or three fit parameters). The performance of localization sequences with respect to outer volume suppression and partial saturation effects may influence the result of relaxation time measurements, e.g., via T_1 -weighting of contamination signals (22), the composition of the tissue in the volume under investigation (i.e., the predominant type of muscle fibers) influences average relaxation times. These factors may explain the relatively wide range of data published for T_1 at 1.5 T, as summarized in Table 3. There appear to be no significant differences between published T_1 s and the values presented here.

Furthermore, T_1 and T_2 may depend on the magnetic field strength and their functional dependence on B_0 may vary between metabolites due to the predominance of different relaxation pathways involved, e.g., dipole-dipole interaction or chemical shift anisotropy relaxation mechanism (23,24).

We proceed to discuss some methodological aspects concerning the estimation of ^{31}P -relaxation times using STEAM localization at 3 T. From a theoretical point of view, inversion recovery is the preferred acquisition scheme for accurate T_1 measurements. However, as this method requires full relaxation of the magnetization before each scan, it is not feasible in vivo, when SNR per unit time is a critical factor and the signal has to be averaged over a large number of scans (up to $\text{NEX} = 512$ for a given TR, in this study). Therefore, bearing in mind the relatively low SNR inherent in localized measurements of ^{31}P metabolites, we used the more time-efficient PS scheme for the T_1 measurements. The estimation of the localization performance in the test object described above proves that

Table 2
 T_2 Relaxation Times (ms) in Human Calf Muscle In Vivo at 3 T

Subject	Gender	P_i	PCr	γ -NTP	α -NTP	β -NTP
1	F	151 ± 25	338 ± 9	72	62	49
6	F	175 ± 22	309 ± 6	82	64	90
7	F	147 ± 15	358 ± 7	89	52	40
3	M	159 ± 20	350 ± 8	75	48	62
8	M	132 ± 10	286 ± 3	59	45	38
9	M	127 ± 11	362 ± 6	89	57	52
Mean \pm SD		148 ± 17	334 ± 30	78 ± 13	55 ± 7	55 ± 10

Errors given for each subject are individual standard deviations returned by the relaxation time fit routine for the singlet resonances. Also shown are the standard deviations of T_2 over all subjects.

Table 3
 T_1 and T_2 Relaxation Times of Human Calf Muscle

T_1/T_2	Method	n	Ref.	B_0 (T)	P_i	PCr	γ -NTP	α -NTP	β -NTP
T_1 (s)	IR-ISIS	1	(31)	1.5	5.3 ± 0.5	6.9 ± 0.6	5.0 ± 0.5	3.2 ± 0.5	4.1 ± 0.4
T_1 (s)	IR	5	(6)	1.5	4.0 ± 0.9	5.5 ± 0.2	4.7 ± 0.5	3.6 ± 0.5	4.3 ± 0.6
T_1 (s)	SR	7	(5)	1.5	4.7 ± 0.3	6.5 ± 0.7	4.2 ± 1.3	3.9 ± 0.6	4.1 ± 1.3
T_1 (s)	SR	23	(3)	1.5	3.5 ± 0.4	5.0 ± 0.6	4.1 ± 0.4	2.9 ± 0.5	3.6 ± 0.3
T_1 (s)	IR	11	(4)	1.5	4.2 ± 0.5	6.1 ± 0.3	4.6 ± 0.3	3.2 ± 0.5	3.7 ± 0.6
T_1 (s)	PS ^a	11	(4)	1.5	4.0 ± 0.5	5.6 ± 0.5	4.5 ± 0.4	3.4 ± 0.6	3.8 ± 0.8
T_1 (s)	2-angle	8	(12)	2.0	5.4 ± 1.7	6.0 ± 0.5	3.5 ± 1.0	3.9 ± 0.8	3.9 ± 0.8
T_1 (s)	IR	8	(12)	2.0	4.6 ± 0.5	6.5 ± 1.1	4.8 ± 0.6	3.5 ± 0.6	3.6 ± 0.8
T_1 (s)	fast IR ^{b1}	6	(13)	2.35	$(7.6 \pm 0.8)^c$	6.6 ± 0.4	3.7 ± 0.3	3.0 ± 0.2	3.5 ± 0.4
T_1 (s)	fast IR ^{b2}	6	(13)	2.35	6.5 ± 0.5	6.5 ± 0.3	4.9 ± 0.4	3.3 ± 0.2	4.1 ± 0.2
T_1 (s)	STEAM ^a	5	this work	3.0	5.2 ± 1.0	6.4 ± 0.2	4.5 ± 0.3	2.6 ± 0.9	3.5 ± 1.1
T_2 (ms)	SE ^d	6	(7)	1.5	205 ± 14	424 ± 21	$(16 \pm 5)^d$	$(22 \pm 6)^d$	$(8 \pm 2)^d$
T_2 (ms)	SE/sel E ^e	12	(8)	1.5	240 ± 48	425 ± 21	93 ± 3^e	74 ± 1^e	75 ± 2^e
T_2 (ms)	SE ^f	16	(9)	1.5	—	—	61	66	69
T_2 (ms)	sel E ^e	16	(9)	1.5	—	—	95	74	75
T_2 (ms)	STEAM	6	this work	3.0	148 ± 17	334 ± 30	78 ± 13	55 ± 7	55 ± 10

^aProgressive saturation.

^{b1} $T_1 = 2.65$ s.

^{b2} $T_1 = 5.15$ s.

^cOverestimated due to low SNR.

^dSpin echo, phase modulation not taken into account.

^eSelective echo, 90° - $T_E/2$ - 2662 - $T_E/2$ - acq scheme.

^fValue at $T_E = 1/J$ (signal loss due to B_1 inhomogeneity).

the VOI was well defined. Measurements on a homogeneous phantom using different voxel sizes demonstrated that measured T_1 relaxation times were not degraded by B_1 inhomogeneity. The average deviation from full saturation of the initial magnetization $S(\text{TR} \rightarrow 0)$, obtained via a three-parameter fit routine, was as low as 3.0% for PCr in the in vivo study. The average deviations from ideal saturation for P_i , γ -NTP, α -NTP, and β -NTP were 4.1%, 5.4%, 12.1%, and 13.9%, respectively (see Fig. 3).

One should also bear in mind that the parameter T_1 of PCr and γ -NTP, obtained from a progressive saturation experiment, is not the “true” or intrinsic longitudinal relaxation time T_1 , as these metabolites undergo chemical exchange. It rather represents an “apparent” T_1 relaxation time (25,26), and there has been discussion whether this fact impedes the use of monoexponential functions to correct for saturation or whether chemical exchange effects can be neglected (27). However, the introduction of additional fit parameters appears to be inappropriate, given our data quality and number of data points, as the single exponential functions appear to model the relaxation behavior very well, particularly for PCr.

Although variation of TM was shown to be a feasible method for measuring T_1 (28), the influence of $\text{TM} = 30$ ms on the results of T_1 fits was neglected in our study, as TM was far shorter than the minimum TR of the PS experiments.

Transverse relaxation times of uncoupled nuclei were measured by fitting an exponential function to signal intensities of spectra acquired at a number of echo times. The decreasing SNR at longer echo times may induce a systematic error in the evaluation of T_2 , as the signal intensity tends to be overestimated when the signal decays to noise level, even if automated fit routines are used for spectral quantification. To compensate for this error, the

number of averages was increased at long TEs and the noise level was taken into account for weighting in the relaxation time fit routines. For PCr, the SNR was sufficient to avoid this effect, although for P_i it may lead to a slight overestimation of T_2 (see Fig. 4).

Homonuclear J -coupling of the ^{31}P nuclei in NTP causes a TE-dependent phase modulation of the NMR signals, which can be suppressed using frequency-selective spin echoes (9). The estimation of T_2 using the signal acquired with STEAM at only two echo times, spaced according to the phase modulation, is less accurate than the aforementioned approach. A reasonable estimate of T_2 could, however, still be achieved.

The quality of the T_1 and T_2 fits, given as correlation coefficients r^2 , is excellent for PCr and acceptable for the less abundant, i.e., lower SNR, metabolites in resting muscle tissue.

Comparison with the limited T_2 data available at 1.5 T suggests a lower T_2 at 3 T, although the 1.5 T data available are quite scattered (7,8), as shown in Table 3. Anomalous relaxation behavior has also been observed in proton spectra of human brain metabolites (29,30), where dipole-dipole relaxation is supposed to dominate relaxation. Some factors possibly contributing to the decrease of T_2 with increasing B_0 have been discussed in the literature, e.g., diffusion in local gradients related to susceptibility differences or dipole-dipole interaction with paramagnetic substances (29).

In conclusion, localized ^{31}P -MRS at 3 T allows accurate measurements of PCr relaxation times in vivo and, in the resting muscle, results in reasonable estimates for other metabolites. The results presented will be useful for absolute quantification of phosphorus metabolites in healthy subjects.

ACKNOWLEDGMENTS

We thank Vladimir Mlynárik (Vienna, Austria) and Graham J. Kemp (Liverpool, UK) for stimulating discussions. We also thank the anonymous reviewers for detailed comments and suggestions.

REFERENCES

- Heerschap A, Houtman C, in 't Zandt H, van den Bergh A, Wieringa B. Introduction to in vivo ³¹P magnetic resonance spectroscopy of (human) skeletal muscle. *Proc Nutr Soc* 1999;58:861–870.
- Kemp GJ, Radda GK. Quantitative interpretation of bioenergetic data from ³¹P and ¹H magnetic resonance spectroscopic studies of skeletal muscle: an analytical review. *Magn Reson Q* 1994;10:43–63.
- Brown TR, Stoyanova R, Greenberg T, Srinivasan R, Murphy-Boesch J. NOE enhancements and *T*₁ relaxation times of phosphorylated metabolites in human calf muscle at 1.5 Tesla. *Magn Reson Med* 1995;33:417–421.
- Newcomer BR, Boska MD. *T*₁ measurements of ³¹P metabolites in resting and exercising human gastrocnemius/soleus muscle at 1.5 Tesla. *Magn Reson Med* 1999;41:486–494.
- Buchthal SD, Thoma WJ, Taylor JS, Nelson SJ, Brown TR. In vivo *T*₁ values of phosphorus metabolites in human liver and muscle determined at 1.5 T by chemical shift imaging. *NMR Biomed* 1989;2:298–304.
- Thomsen C, Jensen KE, Hendriksen O. In vivo measurements of *T*₁ relaxation times of ³¹P-metabolites in human skeletal muscle. *Magn Reson Imag* 1989;7:231–234.
- Thomsen C, Jensen KE, Hendriksen O. ³¹P NMR measurements of *T*₂ relaxation times of metabolites in human skeletal muscle in vivo. *Magn Reson Imag* 1989;7:557–559.
- Jung WI, Straubinger K, Bunse M, Schick F, Kuper K, Dietze G, Lutz O. ³¹P transverse relaxation times of the ATP NMR signals of human skeletal muscle in vivo. *Magn Reson Med* 1992;28:305–310.
- Straubinger K, Jung WI, Bunse M, Lutz O, Kuper K, Dietze G. Spin-echo methods for the determination of ³¹P transverse relaxation times of the ATP NMR signals in vivo. *Magn Reson Imag* 1994;12:121–129.
- Roth K, Hubsch B, Meyerhoff DJ, Naruse S, Gober J, Lawry T, Boska MD, Matson G, Weiner M. Noninvasive quantitation of phosphorus metabolites in human tissue by NMR spectroscopy. *J Magn Reson* 1989;81:299–311.
- van Ormondt D, de Beer R, Marien AJH, den Hollander JA, Luyten PR, Vermeulen JWAH. 2D approach to quantification of inversion-recovery data. *J Magn Reson* 1990;88:652–659.
- Bottomley PA, Ouwkerk R. Fast sensitive *T*₁ measurement in vivo with low angle adiabatic pulses: the dual-angle method. *J Magn Reson Ser B* 1994;104:159–167.
- Gruetter R, Boesch C, Martin E, Wüthrich K. A method for rapid evaluation of saturation factors in in vivo surface coil NMR spectroscopy using *B*₁-insensitive pulse cycles. *NMR Biomed* 1990;3:265–271.
- Bruhn H, Frahm J, Gyngell ML, Merboldt KD, Haenicke W, Sauter R. Localized proton NMR spectroscopy using stimulated echoes: application to human skeletal muscle in vivo. *Magn Reson Med* 1991;17:82–94.
- Mlynárik V, Gruber S, Starčuk Z, Starčuk Z Jr, Moser E. Very short echo time proton MR spectroscopy of human brain with a standard transmit/receive surface coil. *Magn Reson Med* 2000;44:964–967.
- Bovéé WMMJ, Barbiroli B, de Certaines JD, Howe F, Henriksen O, Keevil SF, Leach MO, Longo R, Podo F, Redmond O, Smith M. Workgroup meeting in quality assessment in MRS, Rome (I), 1990. Report on test objects and procedures. In: Podo F, Orr JS, editors. *Tissue characterization by magnetic resonance spectroscopy and imaging*. Rome: Istituto Superiore di Sanità; 1992. p 129–132.
- Gruetter R. Automatic, localized in vivo adjustment of all first- and second-order shim coils. *Magn Reson Med* 1993;29:804–811.
- Vanhamme L, van den Boogaart A, van Huffel S. Improved method for accurate and efficient quantification of MRS data with use of prior knowledge. *J Magn Reson* 1997;129:35–43.
- van den Boogaart A, van Hecke P, van Huffel S, Graveron-Demilly D, van Ormondt D, de Beer R. MRUI: a graphical user interface for accurate routine MRS data analysis. In: *Book of Abstracts: 13th Annual Meeting of the European Society for Magnetic Resonance in Medicine and Biology*, vol. 4. Prague; 1996. p 318.
- Evelhoch JL, Ackerman JH. NMR *T*₁ measurements in inhomogeneous *B*₁ with surface coils. *J Magn Reson* 1983;53:52–64.
- Albrand JP, Remy C, Benabid AL, Decors M, Jacrot M, Riondel J, Foray MF. ³¹P NMR measurements of *T*₂ relaxation times of ATP with surface coils: suppression of J modulation. *Magn Reson Med* 1986;3:941–945.
- Keevil SF, Newbold MC. The performance of volume selection sequences for in vivo NMR spectroscopy: implications for quantitative MRS. *Magn Reson Imag* 2001;19:1217–1226.
- Evelhoch JL, Ewy CS, Siegfried BA, Ackerman JJ, Rice DW, Briggs RW. ³¹P spin-lattice relaxation times and resonance linewidths of rat tissue in vivo: dependence upon the static magnetic field strength. *Magn Reson Med* 1985;2:410–417.
- Mathur-De Vre R, Maerschalk C, Delporte C. Spin-lattice relaxation times and nuclear overhauser enhancement effect for ³¹P metabolites in model solutions at two frequencies: implications for in vivo spectroscopy. *Magn Reson Imag* 1990;8:691–698.
- Gadian DG, Radda GK, Brown TR, Chance EM, Dawson MJ, Wilkie DR. The activity of creatine kinase in frog skeletal muscle studied by saturation-transfer nuclear magnetic resonance. *Biochem J* 1981;194:215–228.
- Horská A, Horský J, Spencer RG. Measurement of spin-lattice relaxation times in systems undergoing chemical exchange. *J Magn Reson* 1994;110:82–89.
- Ouwkerk R, Bottomley PA. On neglecting chemical exchange effects when correcting in vivo ³¹P MRS data for partial saturation. *J Magn Reson* 2001;148:425–435.
- Frahm J, Merboldt KD, Hänicke W. Localized proton NMR spectroscopy using stimulated echoes. *J Magn Reson* 1987;72:502–508.
- Posse S, Cuenod CA, Risinger R, Le Bihan D, Balaban RS. Anomalous transverse relaxation in ¹H spectroscopy in human brain at 4 Tesla. *Magn Reson Med* 1995;33:246–252.
- Mlynárik V, Gruber S, Moser E. Proton *T*₁ and *T*₂ relaxation times of human brain metabolites at 3 Tesla. *NMR Biomed* 2001;14:325–331.
- Luyten PR, Groen JP, Vermeulen JW, den Hollander JA. Experimental approaches to image localized human ³¹P NMR spectroscopy. *Magn Reson Med* 1989;11:1–21.